Vibrational Relaxation in Liquid Phenylacetylene. 1

ARTICLE *in* THE JOURNAL OF PHYSICAL CHEMISTRY A · FEBRUARY 1998

Impact Factor: 2.69 · DOI: 10.1021/jp9732468

3 AUTHORS, INCLUDING:

H. Abramczyk
Lodz University of Technology
79 PUBLICATIONS **792** CITATIONS

SEE PROFILE

Vibrational Relaxation in Liquid Phenylacetylene. 1

M. Kołodziejski, G. Waliszewska, and H. Abramczyk*

Technical University, Institute of Applied Radiation Chemistry, 93-590 Łódź, Wróblewskiego 15, Poland

Received: October 6, 1997; In Final Form: December 4, 1997

Raman and IR spectra of phenylacetylene dissolved in methylcyclohexane and acetonitrile have been recorded. The IR line widths and Raman isotropic line widths of totally symmetric A_1 vibrations of phenylacetylene—the stretching mode of the ethynyl group C≡C (ν_S(C≡C)), the phenyl ring in-plane stretching (ν_{8a}), the C-phenyl group stretching (ν_S(C−Ph)), and the phenyl ring breathing (mixed with trigonal vibration) (ν_{12})—have been recorded. The spectra have been measured as a function of concentration at room temperature. Theoretical models of vibrational dephasing have been tested and compared with experiment.

1. Introduction

Phenylacetylenes offer a broad range of electronic structures on going from the ground state S_0, to electronically excited states S_1 and T_1, and further to the radical ions $R^{\bullet-}$ and $R^{\bullet+}$. The time-resolved resonance Raman spectra of the radical cation $R^{\bullet+}$, radical anion $R^{\bullet-}$, and triplet state T_1 of diphenylacetylene have been reported recently.[1] These investigations are very important because they help to find correlations between the vibrational properties and electronic changes that are of particular interest with regard to the physical and chemical properties of photoinduced electron-transfer processes.

Some of phenylacetylenes are of particular interest with regard to the most recent liquid crystal technology, namely, polymer-dispersed liquid crystals (PDLCs). The PDLC technology uses fluorinated diphenylacetylene to achieve high-purity nematic materials. Although the PDLC-type displays have not yet reached use in a commercial product, they offer the potential for substantial improvements in the brightness of projection television and other display devices.

The purpose of this paper is to obtain an understanding of vibrational relaxation mechanisms in phenylacetylene liquid solutions at the molecular level. In this article we will show that an intercomparison of Raman and IR intensities, band shapes, and solvent effects for the ethynyl group sensitive vibrations and phenyl ring vibrations in a variety of solvents at different concentrations can provide valuable clues about the contribution to the line width from short-range, hard-sphere repulsive interactions and attractive, long-range electrostatic vibrational dephasing mechanisms. As far as we know, the vibrational dynamics of phenylacetylene has never been reported before.

2. Experimental Section

The totally symmetric A_1 vibrations of phenylacetylene—the stretching mode of the ethynyl group C≡C (ν_S(C≡C)), the phenyl ring in-plane stretching (ν_{8a}), the C-phenyl group stretching (ν_S(C−Ph)), and the phenyl ring breathing (mixed with trigonal vibration) (ν_{12})—have been recorded. The vibrational numbers and description are from ref 2. The Raman spectra were measured with a Ramanor U 1000 (Jobin Yvon) as a function of concentration in methylcyclohexane and acetonitrile at room temperature. As an incident light source we used an argon ion laser at 514 nm (Spectra Physics, model 2017). The interference filter was used to purify the laser line by removing additional natural emission lines which interfere with the Raman lines. The IR spectra of phenylacetylene were measured with Specord M80 (Carl Zeiss, Jena) as a function of methylcyclohexane concentration. The spectral width of the monochromator was 1 cm^{-1} for both Raman and IR spectroscopy. Spectrograde phenylacetylene, methylcyclohexane, and acetonitrile (Aldrich) were used without further purification. A polarization analyzer and scrambler were used to select and record polarized (VV) and depolarized (VH) components of the scattered light. The isotropic Raman spectra were calculated according to the relation

$$I_{iso} = I_{VV} - \frac{4}{3} I_{VH} \tag{1}$$

3. Results

In this section, we present the results of Raman and IR studies on vibrational dynamics in phenylacetylene as a function of concentration in polar and nonpolar solvents. The study of isotropic Raman band widths provides a direct probe of vibrational relaxation (mainly vibrational dephasing), while the IR band width may be affected by both rotational and vibrational relaxation. In many cases the combined Raman and IR studies may provide additional information about mechanisms of vibrational dephasing and reorientational relaxation.

Figure 1a,b shows the VV, VH, and isotropic Raman spectra components and IR spectrum of the stretching mode ν_S(C≡C) of phenylacetylene in methylcyclohexane. The bands are slightly asymmetric on the low-frequency side and were fitted with two or three bands. The best fits both for the isotropic Raman and for the IR bands were obtained with three Gaussian bands with the maximum peak positions at 2106.5, 2112.1, and 2115.6 cm^{-1} (Raman) and 2104.0,2110.2, and 2114.2 cm^{-1} (IR).

In Figure 2 the isotropic Raman and IR maximum peak positions ν_0 of the stretching mode ν_S(C≡C) of phenylacetylene in methylcyclohexane are shown as a function of phenylacetylene mole fraction x_{PA}. The maximum peak positions decrease significantly with increasing phenylacetylene concentration. The Raman shift is 6.37 cm^{-1} on going from $x_{PA} = 0.0$ to $x_{PA} = 1.0$. The concentration dependence of the isotropic Raman peak position was fitted with the linear equation $\nu_0(cm^{-1}) = 2116.14$

S1089-5647(97)03246-X CCC: $15.00
Published on Web 02/20/1998

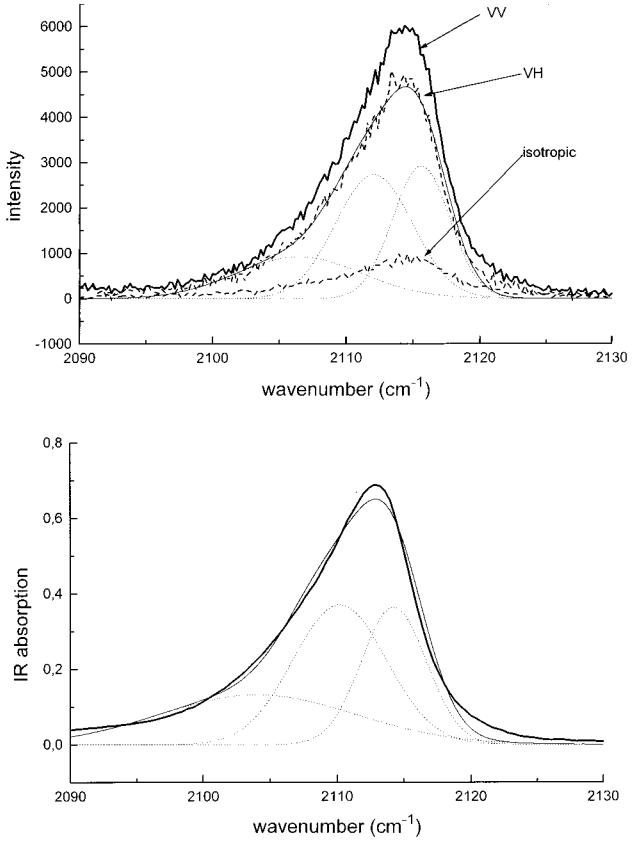

Figure 1. (a) VV, VH, and isotropic Raman spectra of the stretching mode ν_S(C≡C) of phenylacetylene in methylcyclohexane (concentration of phenylacetylene is $c_{PA} = 2.59$ mol/dm^3, $x_{PA} = 0.274$). (b) IR spectra of the stretching mode ν_S(C≡C) of phenylacetylene in methylcyclohexane (concentration of phenylacetylene is $c_{PA} = 2.59$ mol/dm^3, $x_{PA} = 0.274$).

$- 6.37x_{PA}$. The maximum peak position of the anisotropic Raman band (VH) for the stretching mode ν_S(C≡C) of phenylacetylene in methylcyclohexane (not shown in Figure 2) changes in a similar way, and the best fit of the experimental VH data was obtained for the linear equation $\nu_0(\text{cm}^{-1}) = 2116.23 - 5.59x_{PA}$. The maximum peak position of the IR band is decribed by the equation $\nu_0(\text{cm}^{-1}) = 2114.22 - 4.37x_{PA}$.

In contrast, the maximum peak positions of the other studied modes depend very slightly on concentration and were fitted with the following equations. ν_{8a}: $\nu_0(\text{cm}^{-1}) = 1600.27 - 0.57x_{PA}$. ν_S(C−Ph): $\nu_0(\text{cm}^{-1}) = 1195.08 - 1.44x_{PA} + 2.22x_{PA}^2$. ν_{12}: $\nu_0(\text{cm}^{-1}) = 1000.91 - 0.29x_{PA}$.

The data in Figure 2 represent the maximum peak positions ν_0 of the experimental bands. The concentration dependences of the isotropic Raman peak positions of the ν_S(C≡C) band deconvoluted into three Gaussians in the fitting procedure are $\nu_0(\text{cm}^{-1}) = 2109.61 - 3.36x_{PA}$, $\nu_0(\text{cm}^{-1}) = 2114.26 - 4.65x_{PA}$, and $\nu_0(\text{cm}^{-1}) = 2116.46 - 4.13x_{PA}$.

In Figure 3 the the isotropic Raman and IR bandwidths $\Delta_{1/2}$ (fwhh, full width at half-height) of the ν_S(C≡C), ν_{8a}, ν_S(C−Ph), and ν_{12} modes of phenylacetylene in methylcyclohexane are shown as a function of phenylacetylene mole fraction x_{PA}. As we can see, only the bandwidth of the stretching mode ν_S(C≡C) is sensitive to the environment concentration and increases linearly with increasing phenylacetylene mole fraction x_{PA}. The bandwidths $\Delta_{1/2}$ of the ν_S(C≡C) mode in neat phenylacetylene ($x_{PA} = 1.0$) are 10.0 cm^{-1} (isotropic Raman), 10.8 cm^{-1} (anisotropic Raman), and 11.2 cm^{-1} (IR). The concentration dependence of the the isotropic Raman bandwidth $\Delta_{1/2}$ for the ν_S(C≡C) mode was fitted with the linear equation

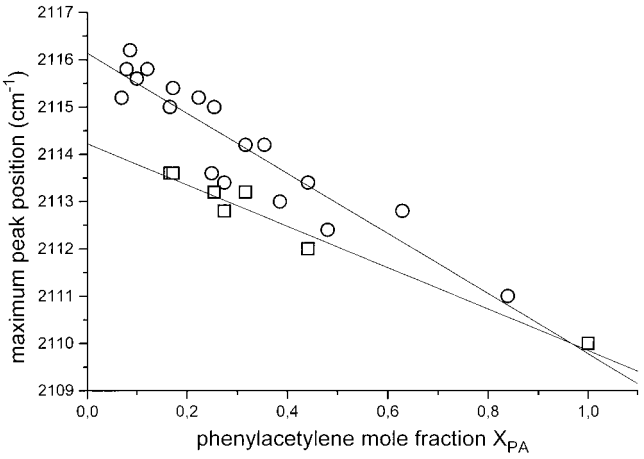

Figure 2. Maximum peak position ν_0 of the stretching mode ν_S(C≡C) of phenylacetylene in methylcyclohexane as a function of phenylacetylene mole fraction x_{PA}: (○) isotropic Raman experimental data ($\nu_0 = 2116.14 - 6.37x_{PA}$); (□) IR data ($\nu_0 = 2114.22 - 4.37x_{PA}$).

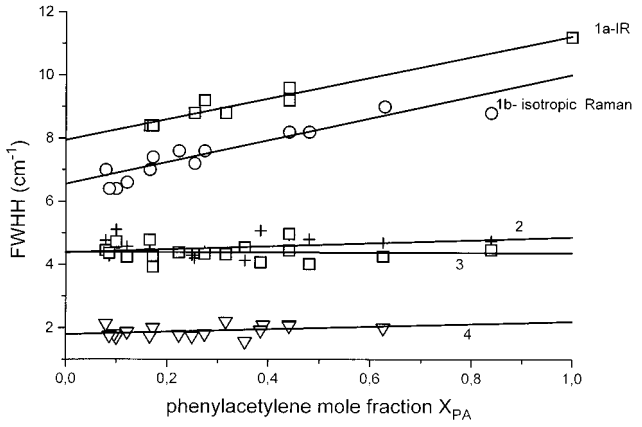

Figure 3. Isotropic Raman bandwidths (fwhh) $\Delta_{1/2}$ of the ν_S(C≡C) (1) (1a, IR data; 1b, isotropic Raman data), ν_S(C−Ph) (2), ν_{8a} (3), and ν_{12} (4) of phenylacetylene in methylcyclohexane as a function of phenylacetylene mole fraction x_{PA}.

$\Delta_{1/2}(\text{cm}^{-1}) = 6.56 + 3.46x_{PA}$. The concentration dependence of the anisotropic Raman (not shown in Figure 3) and IR bandwidths $\Delta_{1/2}$ have similar slopes: $\Delta_{1/2}(\text{cm}^{-1}) = 7.43 + 3.34x_{PA}$ (anisotropic Raman) and $\Delta_{1/2}(\text{cm}^{-1}) = 7.94 + 3.27x_{PA}$ (IR), although the bandwidths are about 1.0−1.5 cm^{-1} broader. This additional broadening is due to reorientational relaxation, which is eliminated in the isotropic bandwidth. The results presented in Figure 3 represent the experimental bandwidths without the deconvolution into three Gaussians. The line widths of the band peaked at 2114.26 cm^{-1} (at $x_{PA} = 0.0$) after deconvolution into three Gaussians are about 1.5 cm^{-1} smaller than the widths in Figure 3.

The bandwidths of the other modes are much narrower, and they practically do not depend on methylcyclohexane concentration. The concentration dependences were fitted with the following equations. ν_{8a}: $\Delta_{1/2}(\text{cm}^{-1}) = 4.39 - 0.027x_{PA}$, ν_S(C−Ph): $\Delta_{1/2}(\text{cm}^{-1}) = 4.38 + 0.48x_{PA}$. ν_{12}: $\Delta_{1/2}(\text{cm}^{-1}) = 1.79 + 0.41x_{PA}$. The results from this section are summarized in Table 1.

4. Discussion

Our results show that vibrational dephasing of the stretching mode ν_S(C≡C) of phenylacetylene is very sensitive to the details of the interaction potential, and it can be used to probe the influence of the solvent effect. The basic question we wish to

TABLE 1: Best-Fit Equations of the Experimental Data for the Concentration Dependence of Phenylacetylene in Methylcyclohexane as a Function of Phenylacetylene Mode Fraction x_{PA}

type of vibration	peak positions $\nu_0(cm^{-1})$	bandwidths $\Delta_{1/2}(cm^{-1})$
$\nu_S(C\equiv C)$ isotropic Raman	$2116.14 - 6.37x_{PA}$	$6.56 + 3.46x_{PA}$
$\nu_S(C\equiv C)$ anisotropic Raman	$2116.23 - 5.59x_{PA}$	$7.43 + 3.34x_{PA}$
$\nu_S(C\equiv C)$ IR	$2114.22 - 4.37x_{PA}$	$7.94 + 3.27x_{PA}$
ν_{8a}	$1600.27 - 0.57x_{PA}$	$4.39 - 0.027x_{PA}$
$\nu_S(C-Ph)$	$1195.08 - 1.44x_{PA} + 2.22x_{PA}^2$	$4.38 + 0.48x_{PA}$
ν_{12}	$1000.91 - 0.29x_{PA}$	$1.79 + 0.41x_{PA}$

address is why the stretching mode $\nu_S(C\equiv C)$ of phenylacetylene relaxes much faster than the other modes.

Here, we will consider whether the spectroscopic properties of phenylacetylene presented in the above section can be rationalized in terms of the existing literature models of vibrational dephasing. Although the dephasing of molecular vibrations has been the subject of intense theoretical and experimental studies,[3−25] an understanding of the dephasing process in nematic materials is still lacking.

A. Mechanisms of Vibrational Dephasing. The theory of vibrational dephasing has been discussed many times (see reviews in refs 3−6), and we will repeat only necessary details to follow the disscusion more easily. The Raman or IR (neglecting reorientational relaxation) line shape due to dephasing (neglecting population relaxation, interaction-induced effects, vibrational transition of overtones, and cross correlations between vibrations localized on different molecules) is given by the Fourier transform of the normalized vibrational correlation function $\langle Q_k(0)\ Q_k(t)\rangle/\langle Q_k(0)\rangle^2$ expressed as

$$\langle Q_k(0)\ Q_k(t)\rangle/\langle Q_k(0)\rangle^2 = \mathrm{Re}\ \exp(i\omega_0 t)\langle \exp[i\int_0^t \Delta\omega(t')]\ dt'\rangle \quad (2)$$

where ω_0 is the frequency of the isolated oscillator of the specified Q localized on the molecule k and $\Delta\omega$ is the frequency change due to the coupling of the solute oscillator Q_k to the intra- or intermolecular environment:

$$H = H_0 + H_B + V_{intra} + V_{inter} \quad (3)$$

Here H_0 is the Hamiltonian of nonperturbated oscillator Q_k and H_B is the free bath Hamiltonian. The coupling term V can be Taylor expanded in the usual manner:

$$V = \frac{\partial V}{\partial Q_k}Q_k + \frac{\partial^2 V}{\partial Q_k^{\ 2}}\frac{Q_k^{\ 2}}{2} + \frac{1}{2}\sum_l \frac{\partial^2 V}{\partial Q_k\,\partial Q_l}Q_kQ_l = FQ_k + G_1Q_k^{\ 2} + \sum_l G_2Q_kQ_l \quad (4)$$

where summation is performed over molecules l perturbing the vibration Q_k.

Here the forces F, G_1, and G_2 represent the forces linear, quadratic, and bilinear in Q exerted by the inter- and intramolecular interactions along the normal coordinate Q_k. F and G_1 are the part of the coupling Hamiltonian which is diagonal in the eigenfunctions of the H_0 basis set and is called the pure vibrational dephasing. The bilinear term G_2 couples the states that differ only by the permutation of individual molecular eigenfunctions and describes the resonant energy transfer.

To make further progress in application of the vibrational dephasing theory, it is necessary to consider the specific type of interactions that can contribute to the forces F and G.

B. Hard Collision Mechanism of Vibrational Dephasing.[7,14,18] First we have applied a model based on a motionally narrowed collision mechanism of vibrational dephasing[7,10,14] which defines the F and G forces as the repulsive interactions due to hard collisions with solvent molecules. To estimate the contribution from this mechanism to the band broadening of phenylacetylene in liquid solutions, we have used the Fischer−Laubereau model[14] modified for mixtures. The model studies the collinear collision of diatomic AB of mass $m_A + m_B$ with an atom C of mass m_C, using an exponential repulsive potential

$$V(Q,R) = E\exp(\gamma Q/L - R/L) \quad (5)$$

where E is the relative kinetic energy, L is the range of the potential (estimated as the molecular diameter σ devided by 18.0), R is the distance from the atom C of mass m_C to the center-of-mass A−B, and γ is the amplitude factor:

$$\gamma = m_A/(m_A + m_B) \quad (6)$$

Using the potential expressed by eq 5 leads to the final result for the vibrational dephasing time:

$$\tau_{ph} = \frac{2}{9}\tau_c M^2\omega_0^{\ 2}L^2/\mu\gamma^4 kT \quad (7)$$

where

$$\mu = \frac{m_C(m_A + m_B)}{m_A + m_B + m_C} \quad (8)$$

The τ_c^{-1} is the hard-sphere collision rate taken as the Enskog collision rate τ_E^{-1}:[7]

$$\tau_c^{-1} = \tau_E^{-1} = \frac{8}{3}\left(\frac{\pi kT}{2m}\right)^{1/2}\rho\sigma^2 g \quad (9)$$

where

$$m^{-1} = m_c^{-1} + M^{-1}$$

Some authors[19] take $\tau_c^{-1} = (3/2)\tau_E^{-1}$ in eq 9 and factor 1/4 instead of 2/9[20] in eq 7. The hard collision bandwidth δ_{ph} consists of the solute−solute (ii) and solute−solvent (ik) collisions:

$$(\delta_{ph})_i = x_i(\delta_{ph})_{ii} + x_k(\delta_{ph})_{ik} \quad (10)$$

where x_i and x_k are the mole fraction of the solute and solvent. The partial bandwidth contributions (full width at half-height) $(\delta_{ph})_{ii}$ and $(\delta_{ph})_{ik}$ can be calculated from combining eqs 7−9.

$$(\delta_{ph})_{ik}(cm^{-1}) = 12\gamma^4(\mu_{ik})(\pi/2)^{1/2}(m^{-1/2})(kT)^{3/2}M^{-2}\omega_0^{\ -2}L_{ik}^{\ -2}\sigma_{ik}^{\ 2}\rho g_{ik}/\pi c \quad (11)$$

where $M = m_Am_B/(m_A + m_B)$ is the reduced mass of the oscillator, $\mu_{ik} = \mu_i\mu_k/(\mu_i + \mu_k)$ is the reduced mass of the colliding molecules, $\mu_i = m_A + m_B$, $\mu_k = m_C$, γ is the amplitude factor, L_{ij} measures the range of interactions between the colliding molecules, ω_0 is the angular frequency of the oscillator M, σ_{ik} is equal to $(\sigma_i + \sigma_k)/2$, where σ_i and σ_k are the hard-sphere diameters, ρ is the number density of the system, g_{ik} is the contact value of the radial distribution function, and c is

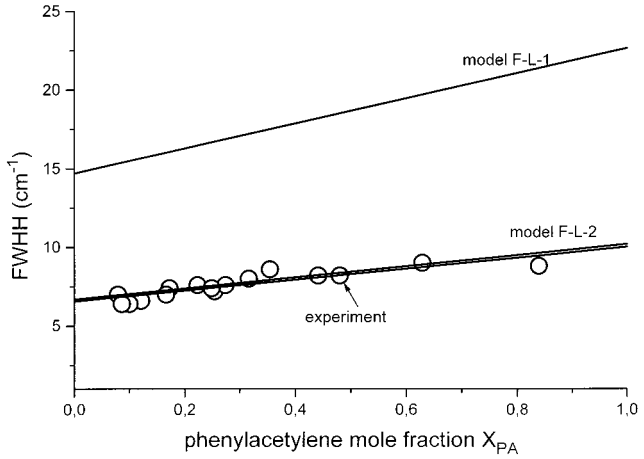

Figure 4. Isotropic Raman bandwidths (fwhh) $\Delta_{1/2}$ of the ν_S(C≡C) of phenylacetylene in methylcyclohexane as a function of phenylacetylene mole fraction x_{PA}: (○) experimental data; (—) theoretical bandwidths calculated from the hard-sphere repulsive model; model F-L-1 ($m^{-1} = m_c^{-1} + M^{-1}$ in eq 9), model F-L-2 ($m = \mu_{ik} = \mu_i\mu_k/(\mu_i + \mu_k)$ in eq 9).

TABLE 2: Parameters Used in the Hard-Sphere Repulsive Model of Vibrational Dephasing for the Phenylacetylene−Methylcyclohexane System

vibrational mode	$M \times 10^{23}$ [g]	γ	$\mu_{ii} \times 10^{23}$ [g]	$\mu_{ik} \times 10^{23}$ [g]
ν_S(C≡C)	1.88	0.8725	8.48	8.31
ν_S(C−Ph)	3.13	0.7549	2.64	2.62
ν_{8a}	3.52	0.7058	2.91	3.01
ν_{12}	3.52	0.7058	2.91	3.01

the light velocity. The other details are explained in the original papers.[7,14] The contact values of the radial distribution functions g_{ik} were calculated from the Percus−Yevick equation[21] as

$$g_{ik}(\sigma_{ik}) = [\sigma_k g_{ii}(\sigma_i) + \sigma_i g_{kk}(\sigma_k)]/2\sigma_{ik} \quad (12)$$

$$g_{ii}(\sigma_i) = \{(1 - \xi) + (3/2)(\sum_{l=1}^{m} \eta_l \sigma_l^2)\sigma_i\}(1 - \xi)^{-2}$$

$$\xi = \sum_{l=1}^{m} \eta_l \sigma_l^3; \quad \eta_l = \pi\rho_l/6 \quad (13)$$

We have used this model for the phenylacetylene−methylcyclohexane system. The parameters used in the calculations are given in Table 2.

The following interaction ranges and the hard-sphere diameters are taken as $L_{ii} = 0.3277$ Å; $L_{ik} = 0.3311$ Å; $\sigma_i = 5.9$ Å; $\sigma_k = 6.02$ Å (i = phenylacetylene, k = methylcyclohexane). We have calculated the bandwidths for the ν_S(C≡C), ν_S(C−Ph), ν_{8a}, and ν_{12} modes of phenylacetylene in methylcyclohexane as a function of concentration using eqs 10−13. The theoretical results for the ν_S(C≡C) mode are shown in Figure 4, where we have compared them with the experimental data. Here, we present the results in two versions, named in this paper as models F-L-1 and F-L-2, respectively. The first one uses the mass factor in eq 9 as $m^{-1} = m_c^{-1} + M^{-1}$,[7] whereas the second takes m, as equal to the reduced mass of colliding molecules ($m = \mu_{ik} = \mu_i\mu_k/(\mu_i + \mu_k)$).[9] Taking into account that the procedure of calculating the reduced mass of the oscillator M is simple only in the case of diatomic molecules, we feel that F-L-2 provides more realistic values of the collision times than F-L-1. Indeed, we can see that the second version (model F-L-2 in Figure 4) gives excellent agreement with experiment for both the bandwidth absolute magnitudes and the slope of the concentration dependence: the experimental data are fitted with the equation $\Delta_{1/2}(\text{cm}^{-1}) = 6.56 + 3.46x_{PA}$, whereas the theoretical model gives $\Delta_{1/2}(\text{cm}^{-1}) = 6.68 + 3.50x_{PA}$. In contrast, the first version (model F-L-1 in Figure 4) gives much worse reproduction: $\Delta_{1/2}(\text{cm}^{-1}) = 14.70 + 7.93x_{PA}$.

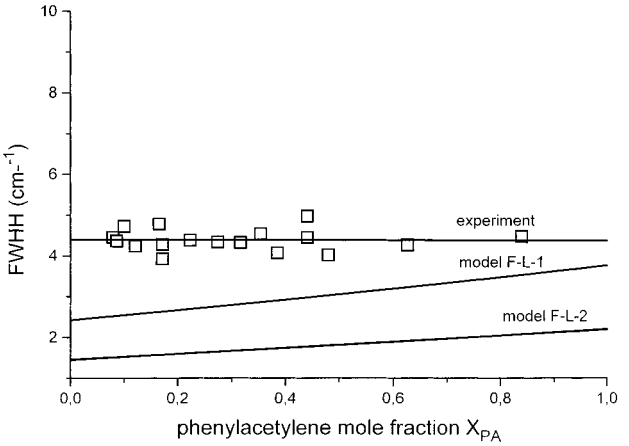

Figure 5. Isotropic Raman bandwidths (fwhh) $\Delta_{1/2}$ of the ν_{8a} of phenylacetylene in methylcyclohexane as a function of phenylacetylene mole fraction x_{PA}: (□) experimental data; (—) theoretical bandwidths calculated from the hard-sphere repulsive model; model F-L-1 ($m^{-1} = m_c^{-1} + M^{-1}$ in eq 9), model F-L-2 ($m = \mu_{ik} = \mu_i\mu_k/(\mu_i + \mu_k)$ in eq 9).

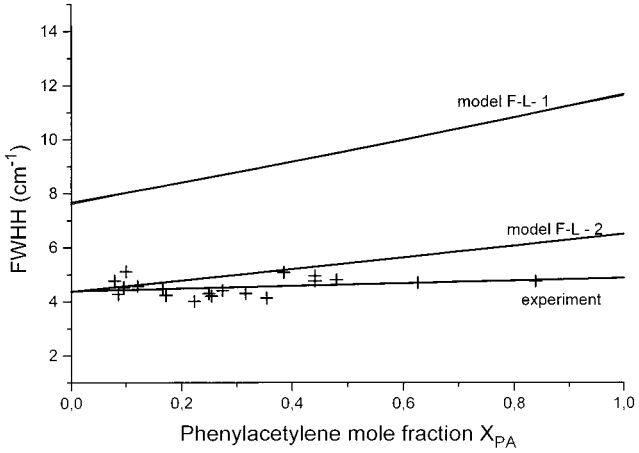

Figure 6. Isotropic Raman bandwidths (fwhh) $\Delta_{1/2}$ of the ν_S(C−Ph) of phenylacetylene in methylcyclohexane as a function of phenylacetylene mole fraction x_{PA}: (+) experimental data, (—) theoretical bandwidths calculated from the hard-sphere repulsive model; model F-L-1 ($m^{-1} = m_c^{-1} + M^{-1}$ in eq 9), model F-L-2 ($m = \mu_{ik} = \mu_i\mu_k/(\mu_i + \mu_k)$ in eq 9).

In Figures 5−7 we show the theoretical results compared with the experimental data for the other modes. We can see that also for the ν_S(C−Ph) mode (Figure 6), the second version of the model reproduces much better the experimental data, giving good agreement with experiment at lower concentration of phenylacetylene. However, the theoretical slope of the concentration dependence is higher than the experimental one: we obtained $\Delta_{1/2}(\text{cm}^{-1}) = 4.38 + 0.48x_{PA}$ from experiment and $\Delta_{1/2}(\text{cm}^{-1}) = 4.35 + 2.14x_{PA}$ from the model (model F-L-2 in Figure 6). The model F-L-1 gives much worse reproduction of the experimental results: $\Delta_{1/2}(\text{cm}^{-1}) = 7.60 + 4.00x_{PA}$.

The results for the vibrations of the phenyl group (Figures 5 and 7) are poorly reproduced by both versions of the model, overestimating (ν_{12} mode, Figure 7) or underestimating (ν_{8a} mode, Figure 5) the experimental data. However, even in these

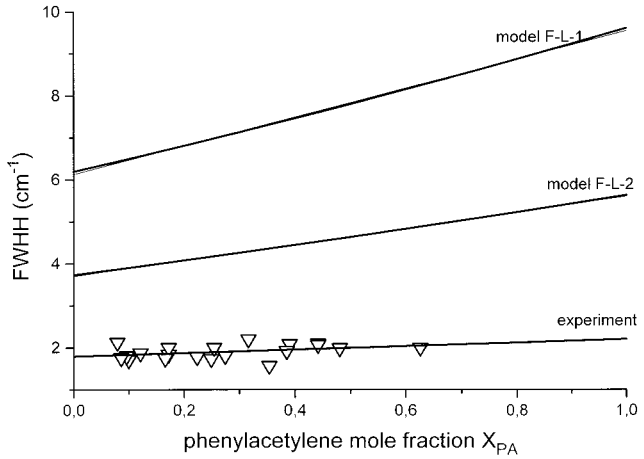

Figure 7. Isotropic Raman bandwidths (fwhh) $\Delta_{1/2}$ of the ν_{12} of phenylacetylene in methylcyclohexane as a function of phenylacetylene mole fraction x_{PA}: (▽) experimental data; (—) theoretical bandwidths calculated from the hard-sphere repulsive model; model F-L-1 ($m^{-1} = m_c^{-1} + M^{-1}$ in eq 9), model F-L-2 ($m = \mu_{ik} = \mu_i\mu_k/(\mu_i + \mu_k)$ in eq 9).

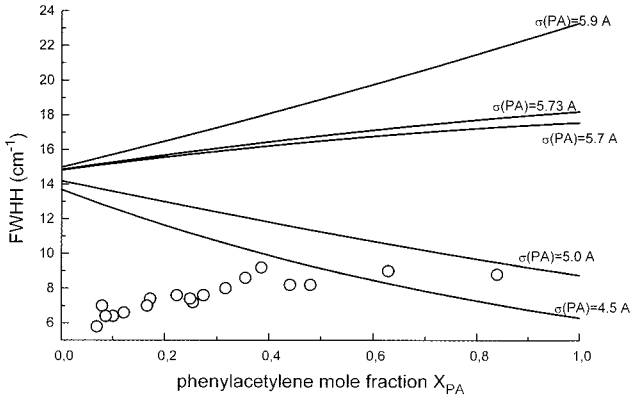

Figure 8. Theoretical isotropic Raman bandwidths (fwhh) $\Delta_{1/2}$ of the ν_S(C≡C) of phenylacetylene in methylcyclohexane as a function of phenylacetylene mole fraction x_{PA} for different hard-sphere diameters of phenylacetylene: (○) experimental data; (—) theoretical bandwidths calculated from the hard-sphere repulsive model for the following hard-sphere diameters of phenylacetylene: σ(PA) = 5.9 Å, σ(PA) = 5.73 Å, σ(PA) = 5.7 Å, σ(PA) = 5.0 Å, σ(PA) = 4.5 Å.

cases, the model F-L-2 gives theoretical slopes of the concentration dependences closer to the experimental ones.

In evaluating the repulsive contribution to vibrational bandwidths, the key quantities are the hard-sphere diameter of the solute and the solvent and the radial distribution functions g_{ik}. We used the Percus−Yevick approximation[21,22] to calculate g_{ik}. There are many other approximations based on the Carnahan−Starling hard-sphere liquid equation of state or the scaled particle theory. Recently, Ben-Amotz et al.[18] compared the effects of the equation of state approximations existing in literature on the corresponding hard fluid distribution functions. They showed that the Percus−Yevick equation of state produces reasonable distribution functions, although the Boublik−Mansoori−Carnahan−Starling-Leland (BMCSL) equation is better. More important than the method used for calculations of the distribution functions are accurate estimates of the hard-sphere diameters of the solute and the solvent. In the absence of accurate independent measurements, the solute and the solvent diameters, σ_i and σ_k, are the only adjustable parameters in the hard-sphere repulsive models of vibrational dephasing. The hard-sphere diameter σ_k of methylcyclohexane equal to 6.02 Å taken in our calculations was obtained with an accuracy of about 1% from the equation of state correlations.[18]

So, the only adjustable parameter in our calculation is the phenylacetylene hard-sphere diameter σ_i. Calculations were performed for several choices of this parameter. In Figure 8 we show the results (model F-L-1) for the following hard-sphere diameters σ_i of phenylacetylene: 5.9, 5.73, 5.70, 5.0, 4.5 Å. We can see that the hard-sphere diameter of phenylacetylene practically does not change the absolute value of the theoretical bandwidth at infinite dilution ($x_{PA} \approx 0.0$) but has a strong effect on the slope of the concentration dependence. At the value of $\sigma_i = 5.73$ Å also the model F-L-1 (like model F-L-2 discussed above) gives the equation describing the theoretical concentration dependence, $\Delta_{1/2}(\text{cm}^{-1}) = 15.01 + 3.37x_{PA}$, with a slope that is in good agreement with the experimental one. However, the absolute values of the theoretical bandwidths calculated from the F-L-1 model are much worse than from the model F-L-2 and about 2 times greater than the experimental widths.

It can be concluded that the hard repulsive collision vibrational dephasing mechanism calculated from the F-L-2 model reproduces band broadening of the ν_S(C≡C) and ν_S(C−Ph) modes as well as the concentration dependences. For the phenyl modes ν_{8a} and ν_{12}, the model underestimates and overestimates, respectively, the experimental values, although even in these cases the theoretical absolute values rather reasonably predict the experimental data. The differences may be due to the fact that it is much more difficult to estimate resonably the amplitude factor γ or the reduced mass M for the phenyl vibrations, which are more obvious for diatomic oscillators such as ν_S(C≡C) and ν_S(C−Ph).

C. Concentration Fluctuation Models.[23,24] Studing binary mixtures, the influence of concentration fluctuations on the bandwidth should be taken into account. The concentration fluctuation models[23,24] are based on this idea and assumes that the spectroscopically active mode of the reference molecule is perturbed by N environmental perturber particles. Each gives a contribution to the spectral function $I(\omega)$:

$$I(\omega) = \sum c_n I_n(\omega) \tag{14}$$

where $I_n(\omega)$ is the Lorentzian band arising from the individual perturber. The individual Lorentzian $I_n(\omega)$ is characterized by two parameters:

$$\hat{\omega}_n = \omega_0 + \frac{1}{2}N\Delta\omega + \frac{1}{2}(2n - N)\Delta\hat{\omega} \tag{15}$$

$$\hat{\gamma}_n = \gamma_0 + \frac{1}{2}N(\Delta\gamma + R) + \frac{1}{2}(2n - N)\Delta\hat{\gamma} \tag{16}$$

where γ_0 and ω_0 are the bandwidth (hwhh) and the frequency in the neat liquid, respectively, $\Delta\omega$ and $\Delta\gamma$ are the difference in frequency and bandwidth for $x = 0.0$ and $x = 1.0$, and R characterizes the concentration fluctuation rate ($R = 0.0$ is a static limit). Detailed discussions of these models can be found in the original papers.[23,24] We have applied the concentration fluctuation model given in ref 23. As $\Delta\omega$ and $\Delta\gamma$ are equal to zero within the experimental error for the ν_S(C−Ph), ν_{8a}, and ν_{12} (see Figure 3), it can be easily shown from that model that R must be equal to zero. It means that phenylacetylene−methylcyclohexane represents the static limit, where concentration fluctuations are too slow to give any contribution to the bandwidth.

D. Electrostatic Models of Vibrational Dephasing.[7,12,25] The results presented above suggest that the hard collision

mechanism of vibrational dephasing gives the main contribution to vibrational line widths of phenylacetylene in methylcyclohexane.

However, our data for the concentration dependence of the maximum peak position of the ν_S(C≡C) mode (Figure 2) suggest that long-range, attractive electrostatic interactions play an important role in the mean frequency of the oscillator. Indeed, the vibrational peak position of the ν_S(C≡C) mode of polar phenylacetylene increases with dilution in nonpolar methylcyclohexane and is described by the relation $\nu_0(\mathrm{cm}^{-1}) = 2116.14 - 6.37x_{PA}$. This situation is similar to that when a liquid-phase molecule enters a gas phase and its vibrational frequencies usually shift upward, because attractive solute−solvent interactions tend to be less competitive with repulsive forces. To illustrate more clearly the competition between the repulsive and attractive forces on the vibrational frequency, we have measured the maximum peak position of phenylacetylene in polar solvent, acetonitrile ($\mu = 3.44$ D), as a function of concentration. The experimental data were fitted with the following equation: $\nu_0(\mathrm{cm}^{-1}) = 2110.43 - 2.13x_{PA}$. We can see that the vibrational frequency at $x_{PA} = 0$ is equal to 2110.43 cm^{-1} in polar acetonitrile, which is remarkably smaller than in nonpolar methylcyclohexane (2116.14 cm^{-1}).

The maximum peak position of the vibrational band in solution is the average $\langle\omega\rangle$ over the frequencies of molecular oscillators in the statistical ensamble, whereas the line width comes from fluctuations in the solute vibrational frequency $\Delta\omega = \omega - \langle\omega\rangle$, due to fluctuations in the solvent−solute interactions. The meaning of these spectral quantities denotes that generally the contributions from attractive and repulsive solvent forces may be different for the frequency shift and the line width.

To examine if the attractive electrostatic interactions give any contribution to the line widths of the studied modes in phenylacetylene, we have tested two electrostatic models: the transition dipole−dipole coupling model (TD−D) and the Onsager model. In the dipole−dipole approximation, one can express the coupling term V_{inter} in eq 3 as

$$V_{inter} = (4\pi\epsilon)^{-1} r^{-3} \sum_l \{\vec{\mu}_k \vec{\mu}_l - 3(\vec{\mu}_k \hat{R})(\vec{\mu}_l \hat{R})\} \quad (17)$$

with $\hat{R} = \vec{r}/r$, $r = |R_k - R_l|$, where μ is the dipole moment of the k and l molecules, and r is the average distance between dipoles. Rewriting eq 17 from Cartesian form to radial and orientational coordinates (Ω_k, Ω_l) with respect to a laboratory-fixed reference system, one gets the following spherical harmonic expansion:

$$V_{inter} = 4(\pi\epsilon)^{-1} \sum_l \mu_k \mu_l r^{-3} A \quad (18)$$

where

$$A = \sum_{m,m'} a^{mm'} Y_1^{\,m}(\Omega_k)\, Y_1^{\,m'}(\Omega_l)\, Y_2^{\,-m-m'}(\Omega_{kl}) \quad (19)$$

with $a^{mm'}$ given as simple numerical factors.[25]

Using the Taylor expansion of the dipole moments with respect to the normal coordinate Q, one gets

$$V_{inter} = (4\pi\epsilon)^{-1} r^{-3} \sum_l \left\{ \mu_k^0 \mu_l^0 + \mu_k^0 \left(\frac{\partial\mu}{\partial Q}\right)_l^0 Q_l + \mu_l^0 \left(\frac{\partial\mu}{\partial Q}\right)_k^0 Q_k + \left(\frac{\partial\mu}{\partial Q}\right)_k^0 \left(\frac{\partial\mu}{\partial Q}\right)_l^0 Q_k Q_l + \mu_l^0 \left(\frac{\partial^2\mu}{\partial Q^2}\right)_k^0 Q_k^2 \right\} A \quad (20)$$

The index zero denotes the values at equilibrium position of the oscillator.

Thus, with the eq 20 the forces F and G from eq 4 have been defined, namely,

$$F = (4\pi\epsilon)^{-1} r^{-3} A \sum_l \mu_l^0 \left(\frac{\partial\mu}{\partial Q}\right)_k^0 \quad (21)$$

$$G_1 = (4\pi\epsilon)^{-1} r^{-3} A \sum_l \mu_l^0 \left(\frac{\partial^2\mu}{\partial Q^2}\right)_k^0 \quad (22)$$

$$G_2 = (4\pi\epsilon)^{-1} r^{-3} 4A \sum_l \left(\frac{\partial\mu}{\partial Q}\right)_k^0 \left(\frac{\partial\mu}{\partial Q}\right)_l^0 \quad (23)$$

In this notation μ_k is the dipole moment of the molecule k at which the normal mode Q_k of interest is localized. The force F gives the band broadening contribution due to the interaction between the permanent dipole μ_l^0 of the solute or solvent molecule and the transition dipole $(\partial\mu/\partial Q)_k^0$ of solute molecule k and corresponds to the pure dephasing. The force G_2 gives the contribution due to the interaction between the transition dipoles of solute molecules and corresponds to the resonant energy transfer mechanism in eq 4.

Considering only the weak coupling limit by truncating a cumulant expansion of eq 2 at second order[3] and using

$$Q_{11} - Q_{00} = \frac{f\hbar}{2m^2\omega_0^{\,3}} \quad \text{and} \quad Q_{11}^{\,2} - Q_{00}^{\,2} = \frac{\hbar}{m\omega_0} \quad (24)$$

for the Hamiltonian H_0 in eq 3 defined by

$$H_0 = \frac{p^2}{2m} + \frac{1}{2}m\omega_0^{\,2}Q^2 + \frac{1}{6}fQ^3 \quad (25)$$

results in

$$\langle Q(0)\, Q(t)\rangle = \langle Q(0)\rangle^2 \,\mathrm{Re}\exp[i(\omega_0 + \langle\omega\rangle t)] \exp\left\{\left[-\frac{1}{2}(fm^{-2}\omega_0^{\,-3})^2 \int_0^t \mathrm{d}t'(t-t')\langle\Delta F(0)\,\Delta F(t')\rangle\right] - \frac{1}{2}(m^{-1}\omega_0^{\,-1}) \int_0^t \mathrm{d}t'(t-t')(\langle\Delta G_1(0)\,\Delta G_1(t')\rangle + \langle\Delta G_2(0)\,\Delta G_2(t')\rangle)\right\} \quad (26)$$

where

$$\Delta F = F - \langle F\rangle; \quad \Delta G_1 = G_1 - \langle G_1\rangle; \quad \Delta G_2 = G_2 - \langle G_2\rangle \quad (27)$$

and ΔF, ΔG_1, and ΔG_2 are given by eqs 21 and 23 at $t = 0$ and t', respectively.

Using the limiting cases,[3] one can get the bandwidth (fwhh in s^{-1} units)

$$\Delta = 2(2\ln 2)^{1/2}\langle\Delta\omega^2\rangle^{1/2} \quad \text{static limit} \quad \langle\Delta\omega^2\rangle^{1/2}\tau_c \gg 1 \quad (28)$$

$$\Delta = 2\langle\Delta\omega^2\rangle\tau_c \quad \text{rapid limit} \quad \langle\Delta\omega^2\rangle^{1/2}\tau_c \ll 1 \quad (29)$$

where the vibrational dephasing $\Delta\omega$ due to the permanent dipole− transition dipole coupling (TD−D) mechanism is given by

$$\Delta\omega = \frac{f}{2m^2\omega_0{}^3}\Delta F \tag{30}$$

$$\Delta\omega = \frac{1}{2m\omega_0}\Delta G_1 \tag{31}$$

The resonant transfer effects on $\Delta\omega$ due to the transition dipole−transition dipole coupling (TD−TD) are given by

$$\Delta\omega = \frac{1}{2m\omega_0}\Delta G_2 \tag{32}$$

E. Application of the Transition Dipole−Dipole (TD−D) and the Onsager Model.[12] We restrict our considerations to the static limit because intermolecular long-range dipole−dipole interactions cannot contribute effectively to rapid modulation in vibrational dephasing. Indeed, the tranlational component (r) and the orientational components (Ω) in eq 18 and 19 are slow in comparison with vibrational dephasing. In the further calculations we neglect the pure dephasing term G_1 describing the interaction between the permanent dipole moment of molecule 1 and the second-order changes in the dipole moment of the molecule k and the resonant energy transfer term G_2.

Substituting eq 30 for eq 28, using the expressions for F (eq 21), neglecting translational diffusion, and using the isotropic rotational diffusion, one can calculate the bandwidth resulting from the TD−D mechanism[15]

$$\delta_{ii} = (2\ln 2)^{1/2}\left(\frac{\partial\mu}{\partial Q}\right)_i \mu_i \frac{1}{2} a f r^{-3/2} M^{-2} \omega_i{}^{-3} (4\pi\epsilon)^{-1}\sqrt{N_i}/\pi c \tag{33}$$

$$\delta_{ik} = (2\ln 2)^{1/2}\left(\frac{\partial\mu}{\partial Q}\right)_i \mu_k \frac{1}{2} a f r^{-3/2} M^{-2} \omega_i{}^{-3} (4\pi\epsilon)^{-1}\sqrt{N_k}/\pi c \tag{34}$$

Here, the indices i and k denote the solute and solvent, respectively. N_i and N_k are the solute and solvent number densities. The factor a is a constant obtained after the averaging procedure over translations (r) and orientations of the permanent dipoles and the transition dipole moments for the quantity A in eq 19. In eqs 33 and 34 we have neglected the broadening due to the terms G_1 and G_2 (eqs 31and 32).

To verify if the TD−D mechanism gives a contribution to the band broadening, we have explored the concentration dependence of the isotropic Raman bandwidth for the ν_S(C≡C) mode of phenylacetylene. The pure vibrational dephasing via transition dipole−dipole (TD−D) leads to the following bandwidth:

$$\delta^{\mathrm{TD-D}} = \delta_{ii} + +\delta_{ik} \tag{35}$$

A qualitative description requires an explicit treatment of the δ_{ik} values in eqs 33 and 34. It is worth emphasizing that most of the parameters in eqs 33 and 34 needed to calculate the theoretical bandwidths of phenylacetylene due to the TD−D mechanism can be estimated from the experimental data. Indeed, we can calculate the transition dipole moment of phenylacetylene $(\partial\mu/\partial Q)_i$ from our IR data and from the relation

$$\left(\frac{\partial\mu}{\partial Q}\right)_i = \pm\left(\frac{3c^2 10^3}{\pi N_A} M\epsilon\right)^{1/2} \tag{36}$$

where M is the reduced mass of the oscillator and ϵ is the molar integral extinction coefficient (ϵ[(mol dm^{-3} cm^{-2})$^{-1}$] = $1/cl\int A(\bar{\nu})\,d\bar{\nu}$; $A = \ln(I_0/I)$ is the IR absorption, $\bar{\nu}$ is the wavenumber in cm^{-1}). The molar extinction coefficient ϵ for the ν_S(C≡C) mode of phenylacetylene obtained from our IR experimental data is 129.25 [(mol dm^{-3} cm^{-2})$^{-1}$].Taking this value and $M = 1.88 \times 10^{-23}$ g, we get $(\partial\mu/\partial Q)_i = 0.58$ D/Å. The other data can be taken from literature; namely, the dipole moments are $\mu_i = 0.78$ D (phenylacetylene), $\mu_k = 0.0$ D (methylcyclohexane), and the relative dielectric constants are $\epsilon = 2.02$ (methylcyclohexane) and 2.98 (phenylacetylene). We have assumed that the dielectric constant ϵ in solution changes linearly with solute mole fraction. The only parameters we still need with which to calculate the bandwidths are the average distance r between dipoles and the anharmonic force constant f.

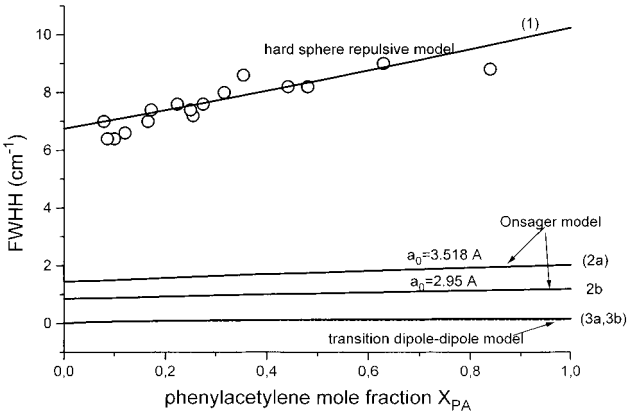

Figure 9. Theoretical isotropic Raman bandwidths (fwhh) $\Delta_{1/2}$ of the ν_S(C≡C) of phenylacetylene in methylcyclohexane as a function of phenylacetylene mole fraction x_{PA} calculated from the hard-sphere repulsive model (1); the Onsager model (2): (2a) $a_0 = 3.518$ Å; (2b) $a_0 = 2.95$ Å; and the transition dipole−dipole coupling model (3): (3a) σ(PA) = 5.9 Å, σ(MCH) = 6.02 Å; (3b) σ(PA) = 7.036 Å, σ(MCH) = 7.053 Å; (○) experimental data.

The anharmonic force constant f can be calculated from the Raman or IR experimental frequencies of the fundamental mode ω_{01} and the first overtone ω_{02}. As the ν_S(C≡C) stretching fundamental mode of phenylacetylene is observed at $\bar{\nu}_{01} = 2109$ cm^{-1}, the first overtone $\bar{\nu}_{02}$ should be expected at about the 4218 cm^{-1} region. Unfortunately, we are not able to observe any band in the region. So, the f value is the only adjustable parameter in our model. We take $f = 36.2 \times 10^{14}$ g cm^{-1} s^{-2}. The average distance r between dipoles was calculated as $r = (\sigma(\mathrm{PA}) + \sigma(\mathrm{MCH}))/2$, where σ(PA) and σ(MCH) are the molecular diameters of phenylacetylene and methylcyclohexane, respectively. For calculations we have taken two sets of diameters: (1) the hard-sphere diameters used in the hard repulsive model of vibrational dephasing, σ(PA) = 5.9 Å and σ(MCH) = 6.02 Å, and (2) the diameters estimated directly from densities, σ(PA) = 7.036 Å and σ(MCH) = 7.053 Å. The diameters from the second version seem to be more appropriate for the long-range attractive interactions.

The theoretical results obtained from the transition dipole−dipole coupling model for the phenylacetylene−methylcyclohexane system are given in Figure 9 and compared with the experimental data and the hard-sphere repulsive model. As we can see, vibrational dephasing via interaction between the solute vibrational dipole and solvent dipole gives a negligible contribution to band broadening. This conclusion is valid for both sets of the molecular diameters. The theoretical TD−D bandwidth of phenylacetylene at infinite dilution is 0.047 cm^{-1} for the first set of diameters and 0.036 cm^{-1} for the second one. To reproduce the absolute values of the experimental data, the anharmonic force constant would have to be about 100 times larger, which does not seem to be reasonable.

Many authors[7,10,18] suggested that the attractive part of the vibrational frequency shift $\Delta\nu_A$ is dominated by dispersive interactions, with a small contribution from inductive forces:

$$\Delta\nu_A = C_A\rho_S = (A_\alpha\alpha_S + A_\mu\mu_S^2)\rho_S \tag{37}$$

where ρ_S is the solvent number density and α_S and μ_S are the polarizability and the dipole moment of the solvent. The constants A_α and A_μ depend primarly on properties of the solute, and they are proportional to the transition polarizability $\partial\alpha/\partial Q$and transition dipole $\partial\mu/\partial Q$, respectively. The first term of eq 39 describes the contribution of dispersion forces, and the second term, the contribution of the dipole−dipole interactions. We showed that the second type of interaction gives a negligible contribution to the line width of phenylacetylene. The theory described by eq 37 predicts the same for the vibrational frequency shift $\Delta\nu_A$ at infinite dilution, because A_μ is proportional to the solvent dipole moment μ_S, which is close to zero for methylcyclohexane. The proper accounting of the contribution to the line width from the dispersive interactions is still lacking.

To develop quantitative predictions for the attractive contribution to the vibrational line width, we proposed recently a simple model based on the Onsager reaction field model.[15] This model produces reasonable predictions for conformationally mobile molecules.

In this model the coupling term V_{inter} in eq 3 describes the interaction between the solute dipole moment μ and the reaction field R and is expressed as

$$V_{inter} = \left[\mu_0 + \left(\frac{\partial\mu}{\partial Q}\right)^0 Q\right]R \tag{38}$$

The Onsager reaction field R is expressed as

$$R = \frac{2(\epsilon - 1)}{2\epsilon + 1}a_0^{-3}\mu \tag{39}$$

where μ is the solute dipole moment, a_0 is the Onsager cavity radius, and ϵ is the dielectric constant. The first term in eq 38 gives the contribution to the frequency shift, and the second term gives the contribution to vibrational dephasing and band broadening. Using the same procedure as for the TD−D model, we can derive the expression for the bandwidth δ^{R-O}(fwhh) due to the interaction between the solute transition dipole ($\partial\mu/\partial Q$)- and dielectric continuum reaction field R:

$$\delta^{R-O}(\mathrm{cm}^{-1}) = (2\ln 2)^{1/2}\left(\frac{\partial\mu}{\partial Q}\right)\mu\frac{1}{2}fM^{-2}\omega^{-3}a_0^{-3}\frac{2(\epsilon - 1)}{2\epsilon + 1}/\pi c \tag{40}$$

We have calculated the theoretical bandwidths δ^{R-O} as a function of phenylacetylene mole fraction x_{PA} and compared with experiment in Figure 9. We have used the following experimental values: $(\partial\mu/\partial Q) = 0.58$ D/Å, $\mu = 0.78$ D, $M = 1.88 \times 10^{-23}$ g, $f = 36.2 \times 10^{14}$ g cm^{-1} s^{-2}, $\omega = 2\pi c(2116.14 - 6.37x_{PA})$. The Onsager cavity radius a_0 was taken as the molecular radius of phenylacetylene estimated above: (1) the hard-sphere diameters used in the hard repulsive model of vibrational dephasing, $a_0 = \sigma(PA)/2 = 5.9/2$ Å $= 2.95$ Å, and (2) the diameter estimated directly from densities, $a_0 = \sigma(PA)/2 = 7.036/2$ Å $= 3.518$ Å. The Onsager model predicts small contributions of about 1 cm^{-1} for $a_0 = 2.95$ Å and 1.5 cm^{-1} for $a_0 = 3.518$ Å, and it does not reproduce the concentration dependence of the line width for the ν_S(C≡C) mode. The theoretical line width dependence from the Onsager model is described by the following equations: $\Delta_{1/2}(\mathrm{cm}^{-1}) = 0.86 + 0.34x_{PA}$ (for $a_0 = 2.95$ Å) and $\Delta_{1/2}(\mathrm{cm}^{-1}) = 1.45 + 0.57x_{PA}$ (for $a_0 = 3.518$ Å) compared with the experimental one: $\Delta_{1/2}(\mathrm{cm}^{-1}) = 6.56 + 3.46x_{PA}$.

5. Conclusions

In this paper we have studied mechanisms of vibrational relaxation of phenylacetylene in methylcyclohexane by Raman and IR band shape analysis. We have found that the vibrational line widths in this system are determined primarily by hard-sphere repulsive collisions. The Fischer−Laubereau model produces reasonable predictions for all the studied modes, but particulary excellent agreement between the experimental data and the theoretical line widths has been obtained for the ν_S-(C≡C) mode. The hard-sphere repulsive collisions model reproduces both the absolute magnitudes and the concentration dependence for this mode, although the long-range, attractive interactions contribute significantly to the vibrational frequency shift of the ν_S(C≡C) mode. This is perhaps not surprising, given that the line widths are determined by dynamic interaction fluctuations, contrary to the shifts that are determined by the average forces.

The long-range, electrostic interactions do not play an important role as a mechanism of band broadening for the vibrational modes of phenylacetylene. We have tested the transition dipole−dipole coupling model (TD−D) and the Onsager reaction field model. The first model (TD−D) assumes that the fluctuations in the interactions between the solute oscillator transition dipole moment ($\partial\mu/\partial Q$) and the solute or solvent permanent dipole moments result in vibrational dephasing and band broadening. The Onsager model has tested the interactions between the transition dipole and the dielectric continuum reaction field. It has been estimated that the broadening due to the TD−D mechanism gives a negligible contribution to the line width. Pure vibrational dephasing due to the Onsager dielectric continuum reaction field contribution still remains unclear. In our calculations it gives contributions of about 1−1.5 cm^{-1}. However, with the more reliable anharmonic force constant f this contribution may change.

The current approach clearly ilustrates that more elaborate methods to estimate the correlation between the mechanisms of vibrational relaxation and the reorganization process from isotropic to partially ordered structures are needed. Additional insight into the line widths and solute−solvent force fluctuations can come from further polarized Raman experiments at low temperatures. The results on vibrational dephasing of phenylacetylene in polar and nonpolar solvents at 77 K will be presented in a subsequent paper.

Acknowledgment. The authors gratefully acknowledge the support of this work by KBN through Grant No. 020/T09/97/12. Support from the Dz.S. 97 is also acknowledged.

References and Notes

(1) Hiura, H.; Takahashi, H. *J. Phys. Chem.* **1992**, *96*, 8909.
(2) Shimojima, A.; Takahashi, H. *J. Phys. Chem.* **1993**, *97*, 9103.
(3) Rotschild, W. G. *Dynamics of Molecular Liquids*; Wiley: New York, 1984.
(4) Oxtoby, D. W. *Annu. Rev. Phys. Chem.* **1981**, *32*, 77.
(5) Laubereau, A.; Kaiser, W. *Rev. Mod. Phys.* **1978**, *50*, 687.
(6) Bratos, S. *Vibrational Spectroscopy of Molecular Liquids and Solids*; Bratos, S., Pick, R. M., Eds.; Plenum: New York, 1980; p 43.
(7) Schweizer, K. S.; Chandler, D. J. *J. Chem. Phys.* **1982**, *76*, 2296.
(8) Schindler, W.; Sharko, P. T.; Jonas, J. *J. Chem. Phys.* **1982**, *76*, 3493.

(9) Tanabe, K.; Jonas, J. *J. Chem. Phys.* **1977**, *67*, 4222.
(10) Ben-Amotz, D.; Lee, M. R.; Cho, S.; List, D. *J. Chem. Phys.* **1992**, *96*, 8781.
(11) Remar, G. J.; Mac Phail, R. A. *J. Chem. Phys.* **1995**, *103*, 4381.
(12) Kołodziejski, M.; Waliszewska, G.; Abramczyk, H. *Chem. Phys.* **1996**, *213*, 341.
(13) Abramczyk, H.; Barut, M.; Ben Altabef, A.; Escribano, R. *J. Phys. Chem.* **1994**, *98*, 424.
(14) Fischer, S. E.; Laubereau, A. *Chem. Phys. Lett.* **1975**, *35*, 6.
(15) Oxtoby, D. W.; Levesque, D.; Weis, J. J. *J. Chem. Phys.* **1978**, *68*, 5528.
(16) Cates, D. A.; Mac Phail, R. A. *J. Phys. Chem.* **1991**, *95*, 2209.
(17) Mac Phail, R. A.; Synder, R. G. *J. Chem. Phys.* **1989**, *91*, 2895.
(18) Ben-Amotz, D.; Herschbach, D. R. *J. Phys. Chem.* **1993**, *97*, 2295.
(19) Tanabe, K. *Chem. Phys.* **1979**, *38*, 131.
(20) Oxtoby, D. W.; Rice, S. A. *Chem. Phys. Lett.* **1976**, *42*, 1.
(21) Lebowitz, J. L. *Phys. Rev.* **1964**, *133*, A895.
(22) Lebowitz, J. L.; Helfand, E.; Praestgard, E. *J. Chem. Phys.* **1965**, *43*, 774.
(23) Knapp, E. W.; Fischer, S. F. *J. Chem. Phys.* **1982**, *76*, 4730.
(24) Miller, L. J.; Vanden Bout, D.; Berg, M. *J. Chem. Phys*. **1993**, *99*, 810.
(25) Van Woerkom, P. C. M.; De Bleyser, J.; De Zwart, M.; Leyte, J. C. *Chem. Phys.* **1974**, *4*, 236.